



# Calculation of predictions for non-identical particle correlations in AA collisions at LHC energies from hydrodynamics-inspired models

MASTER OF SCIENCE THESIS

Author:

**Mateusz Wojciech Gałążyn**

Supervisor:

**Prof. Adam Kisiel**

Warsaw, 3rd August 2014



Obliczenia teoretycznych  
przewidywań korelacji cząstek  
nieidentycznych w zderzeniach  
AA przy energiach LHC  
pochodzących z modeli  
hydrodynamicznych

PRACA MAGISTERSKA

Autor:

**Mateusz Wojciech Gałążyn**

Promotor:

**dr hab. inż. Adam Kisiel, prof. PW**

Warszawa, 3 sierpnia 2014

## **Abstract**

## **Streszczenie**

# Contents

4	<b>1 Theory of heavy ion collisions</b>	<b>2</b>
5	1.1 The Standard Model . . . . .	2
6	1.2 Quantum Chromodynamics . . . . .	3
7	1.2.1 Quarks and gluons . . . . .	3
8	1.2.2 Quantum Chromodynamics potential . . . . .	4
9	1.2.3 The quark-gluon plasma . . . . .	6
10	1.3 Relativistic heavy ion collisions . . . . .	7
11	1.3.1 Stages of heavy ion collision . . . . .	7
12	1.3.2 QGP signatures . . . . .	10
13	<b>2 Terminator model</b>	<b>11</b>
14	2.1 (3+1)-dimensional viscous hydrodynamics . . . . .	11
15	2.2 Statistical hadronization . . . . .	12
16	2.2.1 Cooper-Frye formalism . . . . .	13
17	<b>3 Particle interferometry</b>	<b>15</b>
18	3.1 HBT interferometry . . . . .	15
19	3.2 Intensity interferometry in heavy ion collisions . . . . .	15
20	3.2.1 Theoretical approach . . . . .	15
21	3.2.2 Experimental approach . . . . .	15
22	3.3 Scaling of femtoscopic radii . . . . .	15
23	<b>4 Results</b>	<b>16</b>
24	4.1 Identical particles correlations . . . . .	16
25	4.2 Results of the fit . . . . .	16
26	4.3 Discussion of results . . . . .	16
27	<b>5 Summary</b>	<b>17</b>

# 28 Introduction

# Chapter 1

## Theory of heavy ion collisions

### 1.1 The Standard Model

In the 1970s, a new theory of fundamental particles and their interaction emerged. A new concept, which concerns the electromagnetic, weak and strong nuclear interactions between know particles. This theory is called *The Standard Model*. There are seventeen named particles in the standard model, organized into the chart shown below (Fig. 1.1). Fundamental particles are divided into two families: *fermions* and *bosons*.



Figure 1.1: The Standard Model of elementary particles [1].

Fermions are the building blocks of matter. They are divided into two groups. Six of them, which must bind together are called *quarks*. Quarks are known to bind into doublets (*mesons*), triplets (*baryons*) and recently confirmed four-quark states.<sup>1</sup> Two of baryons, with the longest lifetimes, are forming a nucleus: a proton and a neutron. A proton is build from two up quarks and one down, and neutron consists of two down quarks and one up. A proton is found to be a stable particle (at least it has a lifetime larger than  $10^{35}$  years) and a free neutron has a mean lifetime about  $8.8 \times 10^2$  s. Fermions, that can exist independently are called *leptons*. Neutrinos are a subgroup of leptons, which are only influenced by weak interaction. Fermions can be divided into three generations (three columns in the Figure 1.1). Generation I particles can combine into hadrons with the longest life spans. Generation II and III consists of unstable particles which form also unstable hadrons.

Bosons are force carriers. There are four fundamental forces: weak - responsible for radioactive decay, strong - coupling quarks into hadrons, electromagnetic - between charged particles and gravity - the weakest, which causes the attraction between particles with a mass. The Standard Model describes the first three. The weak force is mediated by  $W^\pm$  and  $Z^0$  bosons, electromagnetic force is carried by photons  $\gamma$  and the carriers of a strong interaction are gluons  $g$ . The fifth boson is a Higgs boson which is responsible for giving other particles mass.

## 1.2 Quantum Chromodynamics

### 1.2.1 Quarks and gluons

Quarks interact with each other through the strong interaction. The mediator of this force is a *gluon* - a massless and chargeless particle. In the quantum chromodynamics (QCD) - theory describing strong interaction - there are six types of "charges" (like electrical charges in the electrodynamics) called *colours*. The colors were introduced because some of the observed particles, like  $\Delta^-$ ,  $\Delta^{++}$  and  $\Omega^-$  appeared to consist of three quarks with the same flavour (*ddd*, *uuu* and *sss* respectively), which was in conflict with the Pauli principle. One quark can carry one of the three colors (usually called *red*, *green* and *blue*) and antiquark one of the three anti-colors respectively. Only color-neutral (or white) particles could exist, mesons are assumed to be a color-anticolor pair, while baryons are *red-green-blue* triplets. Gluons also are color-charged and there are 8 types of gluons. Therefore they can interact with themselves [3].

<sup>1</sup>The LHCb experiment at CERN in Geneva confirmed recently existence of  $Z(4430)$  - a particle consisting of four quarks [2].



## 1.2.2 Quantum Chromodynamics potential

As a result of that gluons are massless, one can expect, that the static potential in the QCD will have the similar form like one in the electrodynamics e.g.  $\sim 1/r$ . In reality the QCD potential is assumed to have the form of [3]

$$V_s = -\frac{4}{3} \frac{\alpha_s}{r} + kr, \quad (1.1)$$

where the  $\alpha_s$  is a coupling constant of the strong force and the  $kr$  part is related with the *confinement*. In comparison to the electromagnetic force, a value of the strong coupling constant is  $\alpha_s \approx 1$  and the electromagnetic one is  $\alpha = 1/137$ .

The fact that quarks does not exist separately, but they are always bound, is called a confinement. As two quarks are pulled apart, the linear part  $kr$  in the eq. 1.1 becomes dominant and the potential becomes proportional to the distance. This situation resembles stretching of a string. At some point, when the string is so large it is energetically favourable to create a quark-antiquark pair. At this moment such pair (or pairs) is formed, the string breaks and the confinement is preserved (Fig. 1.2).

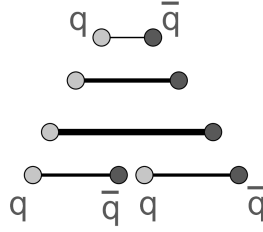


Figure 1.2: A string break and a creation of a pair quark-anti-quark [4].

On the other hand, for the small  $r$ , an interaction between the quarks and gluons is dominated by the Coulomb-like term  $-\frac{4}{3} \frac{\alpha_s}{r}$ . The coupling constant  $\alpha_s$  depends on the four-momentum  $Q^2$  transferred in the interaction. This dependence is presented in Fig. 1.3. The value  $\alpha_s$  decreases with increasing momentum transfer and the interaction becomes weak for large  $Q^2$  ( $\alpha_s(Q) \rightarrow 0$ ). Because of weakening of coupling constant, quarks at large energies (or small distances) are starting to behave like free particles. This phenomenon is known as an *asymptotic freedom*. The QCD potential has also temperature dependence - the force strength “melts” with the temperature increase. Therefore the asymptotic freedom is expected to appear in either the case of high baryon densities (small distances between quarks) or very high temperatures. This temperature dependence is illustrated in the Fig. 1.4.

If the coupling constant  $\alpha_s$  is small, one can use perturbative methods to calculate physical observables. Perturbative QCD (pQCD) successfully describes hard processes (with large  $Q^2$ ), such as jet production in high energy proton-antiproton collisions. The applicability of pQCD is defined by the *scale parameter*



Figure 1.3: The coupling parameter  $\alpha_s$  dependence on four-momentum transfer  $Q^2$  [5].

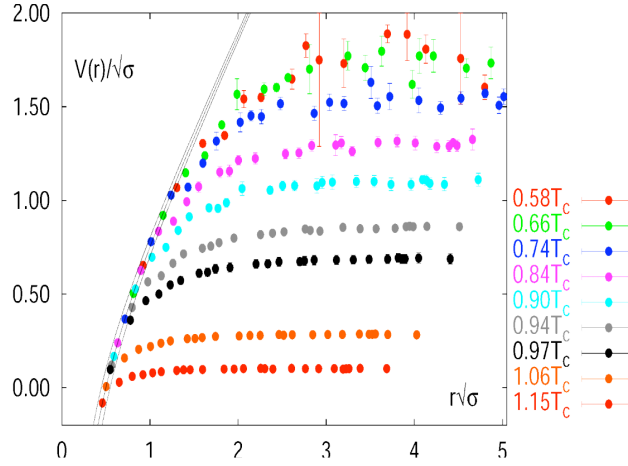


Figure 1.4: The QCD potential for a pair quark-antiquark as a function of distance for different temperatures [4].

101  $\Lambda_{QCD} \approx 200$  MeV. If  $Q \gg \Lambda_{QCD}$  then the process is in the perturbative domain  
 102 and can be described by pQCD. A description of soft processes (when  $Q < 1$  GeV)  
 103 is a problem in QCD - perturbative theory breaks down at this scale. Therefore,  
 104 to describe processes with low  $Q^2$ , one has to use alternative methods like Lattice  
 105 QCD. Lattice QCD (LQCD) is non-perturbative implementation of field theory  
 106 in which QCD quantities are calculated on a discrete space-time grid. LQCD al-  
 107 lows to obtain properties of matter in equilibrium, but there are some limitations.

Lattice QCD requires fine lattice spacing to obtain precise results - therefore large computational resources are necessary. With the constant growth of computing power this problem will become less important. The second problem is that lattice simulations are possible only for baryon density  $\mu_B = 0$ . At  $\mu_B \neq 0$ , Lattice QCD breaks down because of the sign problem [6].

### 1.2.3 The quark-gluon plasma

The new state of matter in which quarks are no longer confined is known as a *quark-gluon plasma* (QGP). The predictions coming from the discrete space-time Lattice QCD calculations reveal a phase transition from the hadronic matter to the quark-gluon plasma at the high temperatures and baryon densities. The res-

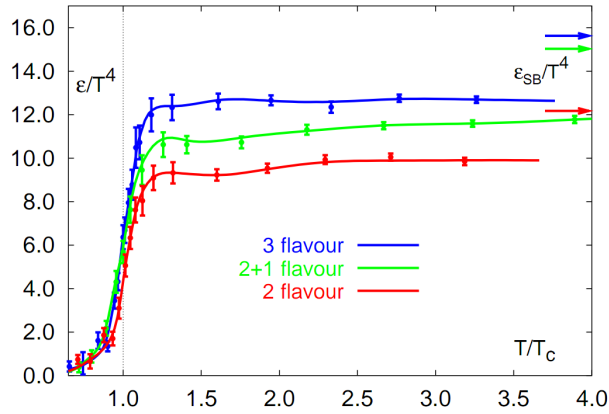


Figure 1.5: A number of degrees of freedom as a function of a temperature [7].

ults obtained from such calculations are shown on Fig. 1.5. The energy density  $\epsilon$  which is divided by  $T^4$  is a measure of number of degrees of freedom in the system. One can observe significant rise of this value, when the temperature increases past the critical value  $T_C$ . Such increase is signaling a phase transition - the formation of QGP [8]. The values of the energy densities plotted in Fig. 1.5 do not reach the Stefan-Boltzmann limit  $\epsilon_{SB}$  (marked with arrows), which corresponds to the ideal gas. This can indicate some residual interactions in the system. According to the results from the RHIC<sup>2</sup>, the new phase of matter behaves more like an ideal fluid, than like a gas [9].

One of the key questions, to which current heavy ion physics tries to find an answer is the value of a critical temperature  $T_C$  as a function of a baryon chemical potential  $\mu_B$  (baryon density), where the phase transition occur. The results coming from the Lattice QCD are presented in the Fig. 1.6. The phase of matter in which quarks and gluons are deconfined is expected to exist at large temperatures. In the region of small temperatures and high baryon densities, a

<sup>2</sup>Relativistic Heavy Ion Collider at Brookhaven National Laboratory in Upton, New York



Figure 1.6: Phase diagram coming from the Lattice QCD calculations [8].

different state is supposed to appear - a *colour superconductor*. The phase transition between hadronic matter and QGP is thought to be of 1<sup>st</sup> order at  $\mu_B \gg 0$ . However as  $\mu_B \rightarrow 0$  quarks' masses become significant and a sharp transition transforms into a rapid but smooth cross-over. It is believed that in Pb-Pb collisions observed at the LHC<sup>3</sup>, the created matter has high enough temperature to be in the quark-gluon plasma phase, then cools down and converts into hadrons, undergoing a smooth transition [8].

### 1.3 Relativistic heavy ion collisions

#### 1.3.1 Stages of heavy ion collision

To create the quark-gluon plasma one has to achieve high enough temperatures and baryon densities. Such conditions can be recreated in the heavy ion collisions at the high energies. The left side of the Figure 1.7 shows simplified picture of a central collision of two highly relativistic nuclei in the centre-of-mass reference frame. The colliding nuclei are presented as thin disks because of the Lorentz contraction. In the central region, where the energy density is the highest, a new state of matter - the quark-gluon plasma - is supposedly created. Afterwards, the plasma expands and cools down, quarks combine into hadrons and their mutual interactions cease when the system reaches the *freeze-out* temperature. Subsequently, produced free hadrons move towards the detectors.

On the right side of the Figure 1.7 there is presented a space-time evolution of a collision process, plotted in the light-cone variables ( $z, t$ ). The two highly relativistic nuclei are traveling basically along the light cone until they collide at the

<sup>3</sup>Large Hadron Collider at CERN, Geneva

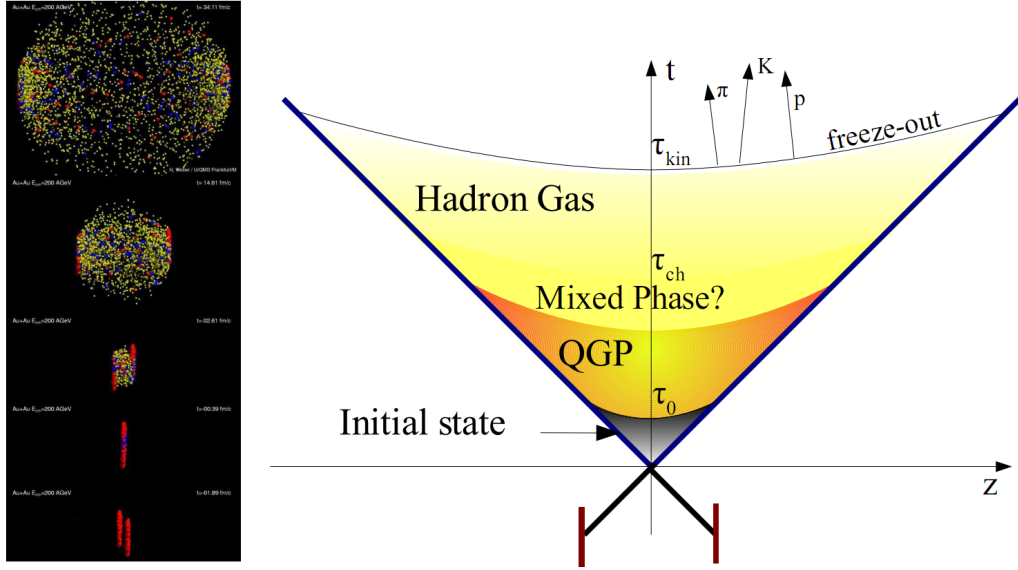


Figure 1.7: Left: stages of a heavy ion collision simulated in the UrQMD model. Right: schematic view of a heavy ion collision evolution [8].

155 centre of diagram. Nuclear fragments emerge from the collision again along the  
 156 (forward) light cone, while the matter between fragmentation zones populates  
 157 the central region. This hot and dense matter is believed to be in the state of the  
 158 quark-gluon plasma. There exist several frameworks to describe this transition to  
 159 the QGP phase, for example: QCD string breaking, QCD parton cascades or color  
 160 glass condensate evolving into glasma and later into quark-gluon plasma [10].

### 161 String breaking

162 In the string picture, the nuclei pass through each other forming color strings.  
 163 This is analogous to the situation depicted in the Fig 1.2 - the color string is cre-  
 164 ated between quarks inside particular nucleons in nuclei. In the next step strings  
 165 decay / fragment forming quarks and gluons or directly hadrons. This approach  
 166 becomes invalid at very high energies, when the strings overlap and cannot be  
 167 treated as independent objects.

### 168 Parton cascade

169 The parton<sup>4</sup> cascade model is based on the pQCD. The colliding nuclei are  
 170 treated as clouds of quarks and which penetrate through each other. The key  
 171 element of this method is the time evolution of the parton phase-space distri-  
 172 butions, which is governed by a relativistic Boltzmann equation with a collision  
 173 term that contains dominant perturbative QCD interactions. The bottleneck of the  
 174 parton cascade model is the low energies regime, where the  $Q^2$  is too small to be

<sup>4</sup>A parton is a common name for quark and gluon.

described by the perturbative theory.

### Color glass condensate

The color glass condensate assumes, that the hadron can be viewed as a tightly packed system of interacting gluons. The saturation of gluons increases with energy, hence the total number of gluons may increase without the bound. Such a saturated and weakly coupled gluon system is called a color glass condensate. The fast gluons in the condensate are Lorentz contracted and redistributed on the two very thin sheets representing two colliding nuclei. The sheets are perpendicular to the beam axis. The fast gluons produce mutually orthogonal color magnetic and electric fields, that only exist on the sheets. Immediately after the collision, i.e. just after the passage of the two gluonic sheets after each other, the longitudinal electric and magnetic fields are produced forming the *glasma*. The glasma fields decay through the classical rearrangement of the fields into radiation of gluons. Also decays due to the quantum pair creations are possible. In this way, the quark-gluon plasma is produced.

Interactions within the created quark-gluon plasma bring the system into the local statistical equilibrium, hence its further evolution can be described by the relativistic hydrodynamics. The hydrodynamic expansion causes that the system becomes more and more dilute. The phase transition from the quark-gluon plasma to the hadronic gas occurs. Further expansion causes a transition from the strongly interaction hadronic gas to weakly interacting system of hadrons which move freely to the detectors. Such decoupling of hadrons is called the *freeze-out*. The freeze-out can be divided into two phases: the chemical freeze-out and the thermal one. The *chemical freeze-out* occurs when the inelastic collisions between constituents of the hadron gas stop. As the system evolves from the chemical freeze-out to the thermal freeze-out the dominant processes are elastic collisions (such as, for example  $\pi + \pi \rightarrow \rho \rightarrow \pi + \pi$ ) and strong decays of heavier resonances which populate the yield of stable hadrons. The *thermal freeze-out* is the stage of the evolution of matter, when the strongly coupled system transforms to a weakly coupled one (consisting of essentially free particles). In other words this is the moment, where the hadrons practically stop to interact. Obviously, the temperatures corresponding to the two freeze-outs satisfy the condition

$$T_{chem} > T_{therm} , \quad (1.2)$$

where  $T_{chem}$  (inferred from the ratios of hadron multiplicities) is the temperature of the chemical freeze-out, and  $T_{therm}$  (obtained from the investigation of the transverse-momentum spectra) is the temperature of the thermal freeze-out [10].

212 **1.3.2 QGP signatures**

213 **Kinematic variables**

214 **Elliptic Flow**

215 **Transverse radial flow**

216 **Direct photon slope**

217 **low-mass dilepton production**

218 **jet quenching**

## 219 Chapter 2

## 220 Terminator model

221 THERMINATOR [11] is a Monte Carlo event generator designed to investigate  
222 the particle production in the relativistic heavy ion collisions. The functionality  
223 of the code includes a generation of the stable particles and unstable resonances  
224 at the chosen hypersurface model. It performs the statistical hadronization which  
225 is followed by space-time evolution of particles and the decay of resonances. The  
226 key element of this method is an inclusion of a complete list of hadronic reson-  
227 ances, which contribute very significantly to the observables. The second version  
228 of THERMINATOR [12] comes with a possibility to incorporate any shape of freeze-  
229 out hypersurface and the expansion velocity field, especially those generated ex-  
230 ternally with various hydrodynamic codes.

### 231 2.1 (3+1)-dimensional viscous hydrodynamics

232 Most of the relativistic viscous hydrodynamic calculations are done in  
233 (2+1)-dimensions. Such simplification assumes boost-invariance of a matter  
234 created in a collision. Experimental data reveals that no boost-invariant region is  
235 formed in the collisions [13]. Hence, for the better description of created system  
236 a (3+1)-dimensional model is required.

237 In the four dimensional relativistic dynamics one can describe a system  
238 using a space-time four-vector  $x^\nu = (ct, x, y, z)$ , a velocity four-vector  
239  $u^\nu = \gamma(c, v_x, v_y, v_z)$  and a energy-momentum tensor  $T^{\mu\nu}$ . The particular  
240 components of  $T^{\mu\nu}$  have a following meaning:

- 241 •  $T^{00}$  - an energy density,
- 242 •  $cT^{0\alpha}$  - an energy flux across a surface  $x^\alpha$ ,
- 243 •  $T^{\alpha 0}$  - an  $\alpha$ -momentum flux across a surface  $x^\alpha$  multiplied by  $c$ ,
- 244 •  $T^{\alpha\beta}$  - components of momentum flux density tensor,



where  $\gamma = (1 - v^2/c^2)^{-1/2}$  is Lorentz factor and  $\alpha, \beta \in \{1, 2, 3\}$ . Using  $u^\nu$  one can express  $T^{\mu\nu}$  as follows [14]:

$$T_0^{\mu\nu} = (e + p)u^\mu u^\nu - pg^{\mu\nu} \quad (2.1)$$

where  $e$  is an energy density,  $p$  is a pressure and  $g^{\mu\nu}$  is an inverse metric tensor:

$$g^{\mu\nu} = \begin{bmatrix} 1 & 0 & 0 & 0 \\ 0 & -1 & 0 & 0 \\ 0 & 0 & -1 & 0 \\ 0 & 0 & 0 & -1 \end{bmatrix}. \quad (2.2)$$

The presented version of energy-momentum tensor (2.1) can be used to describe dynamics of a perfect fluid. To take into account influence of viscosity, one has to apply the following corrections coming from shear  $\pi^{\mu\nu}$  and bulk  $\Pi$  viscosities [15]:

$$T^{\mu\nu} = T_0^{\mu\nu} + \pi^{\mu\nu} + \Pi(g^{\mu\nu} - u^\mu u^\nu). \quad (2.3)$$

The stress tensor  $\pi^{\mu\nu}$  and the bulk viscosity  $\Pi$  are solutions of dynamical equations in the second order viscous hydrodynamic framework [14]. The comparison of hydrodynamics calculations with the experimental results reveal, that the shear viscosity divided by entropy  $\eta/s$  has to be small and close to the AdS/CFT estimate  $\eta/s = 0.08$  [15, 16].

When using  $T^{\mu\nu}$  to describe system evolving close to local thermodynamic equilibrium, relativistic hydrodynamic equations in a form of:

$$\partial_\mu T^{\mu\nu} = 0 \quad (2.4)$$

can be used to describe the dynamics of the local energy density, pressure and flow velocity.

Hydrodynamic calculations are starting from the Glauber<sup>1</sup> model initial conditions. The collective expansion of a fluid ends at the freeze-out hypersurface. That surface is usually defined as a constant temperature surface, or equivalently as a cut-off in local energy density. The freeze-out is assumed to occur at the temperature  $T = 140$  MeV.

## 2.2 Statistical hadronization

Statistical description of heavy ion collision has been successfully used to describe quantitatively *soft* physics, i.e. the regime with the transverse momentum not exceeding 2 GeV. The basic assumption of the statistical approach of evolution of the quark-gluon plasma is that at some point of the space-time evolution of the fireball, the thermal equilibrium is reached. When

<sup>1</sup>The Glauber Model is used to calculate “geometrical” parameters of a collision like an impact parameter, number of participating nucleons or number of binary collisions.

the system is in the thermal equilibrium the local phase-space densities of particles follow the Fermi-Dirac or Bose-Einstein statistical distributions. At the end of the plasma expansion, the freeze-out occurs. The freeze-out model incorporated in the THERMINATOR model assumes, that chemical and thermal freeze-out occur at the same time.

### 2.2.1 Cooper-Frye formalism

The result of the hydrodynamic calculations is the freeze-out hypersurface  $\Sigma^\mu$ . A three-dimensional element of the surface is defined as [12]

$$d\Sigma_\mu = \epsilon_{\mu\alpha\beta\gamma} \frac{\partial x^\alpha}{\partial \alpha} \frac{\partial x^\beta}{\partial \beta} \frac{\partial x^\gamma}{\partial \gamma} d\alpha d\beta d\gamma, \quad (2.5)$$

where  $\epsilon_{\mu\alpha\beta\gamma}$  is the Levi-Civita tensor and the variables  $\alpha, \beta, \gamma \in \{1, 2, 3\}$  are used to parametrize the three-dimensional freeze-out hypersurface in the Minkowski four-dimensional space. The Levi-Civita tensor is equal to 1 when the indices form an even permutation (eg.  $\epsilon_{0123}$ ), to -1 when the permutation is odd (e.g.  $\epsilon_{2134}$ ) and has a value of 0 if any index is repeated. Therefore [12],

$$d\Sigma_0 = \begin{vmatrix} \frac{\partial x}{\partial \alpha} & \frac{\partial x}{\partial \beta} & \frac{\partial x}{\partial \gamma} \\ \frac{\partial y}{\partial \alpha} & \frac{\partial y}{\partial \beta} & \frac{\partial y}{\partial \gamma} \\ \frac{\partial z}{\partial \alpha} & \frac{\partial z}{\partial \beta} & \frac{\partial z}{\partial \gamma} \end{vmatrix} d\alpha d\beta d\gamma \quad (2.6)$$

and the remaining components are obtained by cyclic permutations of  $t, x, y$  and  $z$ .

One can obtain the number of hadrons produced on the hypersurface  $\Sigma^\mu$  from the Cooper-Frye formalism. The following integral yields the total number of created particles [12]:

$$N = (2s + 1) \int \frac{d^3p}{(2\pi)^3 E_p} \int d\Sigma_\mu(x) p^\mu f(x, p), \quad (2.7)$$

where

$$f(p \cdot u) = \left\{ \exp \left[ \frac{p_\mu u^\mu - (B\mu_B + I_3\mu_{I_3} + S\mu_S + C\mu_C)}{T} \right] \pm 1 \right\}^{-1} \quad (2.8)$$

is the phase-space distribution for particles (for stable ones and resonances). For the Fermi-Dirac distribution in the 2.8 there is a plus sign and for Bose-Einstein statistics minus sign respectively. The thermodynamic quantities appearing in the  $f(\cdot)$  are  $T$  - temperature,  $\mu_B$  - baryon chemical potential,  $\mu_{I_3}$  - isospin chemical potential,  $\mu_S$  - strange chemical potential,  $\mu_C$  - charmed chemical potential and the  $s$  is a spin of a particle. One can simply derive from equation 2.7, the dependence of the momentum density [17]:

$$E \frac{dN}{d^3p} = \int f(x, p) p^\mu d\Sigma_\mu. \quad (2.9)$$

299 The equations presented above are directly used in the THERMINATOR to generate  
300 the hadrons with the Monte-Carlo method.

## 301 **Chapter 3**

# 302 **Particle interferometry**

### 303 **3.1 HBT interferometry**

### 304 **3.2 Intensity interferometry in heavy ion collisions**

#### 305 **3.2.1 Theoretical approach**

306 **Two particle wave function**

307 **Source function**

308 **Theoretical correlation function**

309 **Spherical harmonics decomposition of correlation function**

#### 310 **3.2.2 Experimental approach**

### 311 **3.3 Scaling of femtoscopic radii**

## 312 **Chapter 4**

# 313 **Results**

### 314 **4.1 Identical particles correlations**

### 315 **4.2 Results of the fit**

### 316 **4.3 Discussion of results**

<sup>317</sup> **Chapter 5**

<sup>318</sup> **Summary**

# Bibliography

- 320 [1] Standard Model of Elementary Particles - Wikipedia, the free encyclopedia  
321 [http://en.wikipedia.org/wiki/standard\\_model](http://en.wikipedia.org/wiki/standard_model).
- 322 [2] R. Aaij et al. (LHCb Collaboration). Observation of the resonant character of  
323 the  $z(4430)^-$  state. *Phys. Rev. Lett.*, 112:222002, Jun 2014.
- 324 [3] Donald H. Perkins. *Introduction to High Energy Physics*. Cambridge Univer-  
325 sity Press, fourth edition, 2000. Cambridge Books Online.
- 326 [4] G. Odyniec. *Phase Diagram of Quantum Chromo-Dynamics* - course at Faculty  
327 of Physics, Warsaw University of Technology, Jun 2012.
- 328 [5] J. Beringer et al. (Particle Data Group). The Review of Particle Physics. *Phys.*  
329 *Rev.*, D86:010001, 2012.
- 330 [6] Z. Fodor and S.D. Katz. The Phase diagram of quantum chromodynamics.  
331 2009.
- 332 [7] F. Karsch. Lattice results on QCD thermodynamics. *Nuclear Physics A*, 698(1-  
333 4):199 – 208, 2002.
- 334 [8] Adam Kisiel. *Studies of non-identical meson-meson correlations at low relative ve-*  
335 *locities in relativistic heavy-ion collisions registered in the STAR experiment*. PhD  
336 thesis, Warsaw University of Technology, Aug 2004.
- 337 [9] J. Bartke. *Relativistic Heavy Ion Physics*. World Scientific Pub., 2009.
- 338 [10] W. Florkowski. *Phenomenology of Ultra-Relativistic Heavy-Ion Collisions*.  
339 World Scientific, 2010.
- 340 [11] Adam Kisiel, Tomasz Taluc, Wojciech Broniowski, and Wojciech  
341 Florkowski. THERMINATOR: THERMal heavy-IoN generATOR. *Com-*  
342 *put.Phys.Comm.*, 174:669–687, 2006.
- 343 [12] Mikolaj Chojnacki, Adam Kisiel, Wojciech Florkowski, and Wojciech Bro-  
344 niowski. THERMINATOR 2: THERMal heavy IoN generATOR 2. *Com-*  
345 *put.Phys.Comm.*, 183:746–773, 2012.

- 346 [13] I. et al (BRAHMS Collaboration) Bearden. Charged meson rapidity distri-  
347 butions in central Au + Au collisions at  $\sqrt{s_{NN}} = 200$  GeV. *Phys. Rev. Lett.*,  
348 94:162301, Apr 2005.
- 349 [14] W. Israel and J.M. Stewart. Transient relativistic thermodynamics and kin-  
350 etic theory. *Annals of Physics*, 118(2):341 – 372, 1979.
- 351 [15] Piotr Bożek. Flow and interferometry in (3 + 1)-dimensional viscous hydro-  
352 dynamics. *Phys. Rev. C*, 85:034901, Mar 2012.
- 353 [16] K. Kovtun, P. D. T. Son, and A. O. Starinets. Viscosity in strongly interacting  
354 quantum field theories from black hole physics. *Phys. Rev. Lett.*, 94:111601,  
355 Mar 2005.
- 356 [17] Fred Cooper and Graham Frye. Single-particle distribution in the hydro-  
357 dynamic and statistical thermodynamic models of multiparticle production.  
358 *Phys. Rev. D*, 10:186–189, Jul 1974.



359

# List of Figures

360	1.1	The Standard Model of elementary particles [1]. . . . .	2
361	1.2	A string break and a creation of a pair quark-anti-quark [4]. . . . .	4
362	1.3	The coupling parameter $\alpha_s$ dependence on four-momentum transfer $Q^2$ [5]. . . . .	5
363			
364	1.4	The QCD potential for a pair quark-antiquark as a function of distance for different temperatures [4]. . . . .	5
365			
366	1.5	A number of degrees of freedom as a function of a temperature [7].	6
367	1.6	Phase diagram coming from the Lattice QCD calculations [8]. . . .	7
368	1.7	Left: stages of a heavy ion collision simulated in the UrQMD model. Right: schematic view of a heavy ion collision evolution [8].	8
369			